



**HAL**  
open science

## Step-up voltage converter for mems actuators by piezoelectric transformers

François Pigache, Pokorny Marek, Marc Cousineau, Bertrand Nogarède

### ► To cite this version:

François Pigache, Pokorny Marek, Marc Cousineau, Bertrand Nogarède. Step-up voltage converter for mems actuators by piezoelectric transformers. IECON 2009 - 35th Annual Conference of IEEE Industrial Electronics (IECON), Nov 2009, Porto, Portugal. pp.889-894, 10.1109/IECON.2009.5415036 . hal-03284756

**HAL Id: hal-03284756**

**<https://ut3-toulouseinp.hal.science/hal-03284756>**

Submitted on 12 Jul 2021

**HAL** is a multi-disciplinary open access archive for the deposit and dissemination of scientific research documents, whether they are published or not. The documents may come from teaching and research institutions in France or abroad, or from public or private research centers.

L'archive ouverte pluridisciplinaire **HAL**, est destinée au dépôt et à la diffusion de documents scientifiques de niveau recherche, publiés ou non, émanant des établissements d'enseignement et de recherche français ou étrangers, des laboratoires publics ou privés.

# Step-up voltage converter for mems actuators by piezoelectric transformers

Pigache Francois, Pokorny Marek, Cousineau Marc and Nogarede Bertrand  
*Universite de Toulouse; INPT, UPS; LAPLACE (Laboratoire Plasma et Conversion d'Energie);*  
ENSEEIH, 2 rue Charles Camichel, BP 7122, F-31071 Toulouse cedex 7, France  
*{pigache}{cousineau}{nogarede}@laplace.univ-tlse.fr*

**Abstract-** This paper is about the validation of minimal electronic structure developed around piezoelectric transformer for high voltage mems supply. High voltage and compactness are main requirements leading to the development of electronic circuit. The selected solution is discussed and experimentally validated by a first prototype.

## I. INTRODUCTION

IMPROVEMENTS in photolithography techniques and original micro-mechanical structures have led to a new generation of comb-drive actuators able to provide force of some mN. The compactness, low consumption and micro-actuation offer a wide spread of applications such as in surgery, tactile interfaces, clock industry and others. In the case of small embedded systems or easily handle tools, autonomous and compact solutions are necessary. However, these actuators require high voltage supply which can exceed a hundred volts and some kHz of frequency. Currently, the power supply often dominates the overall system size. In consequence, the challenge is to propose a power stage converter satisfying the electrical requirements and dimensions in conformity with actuator size.

Among the solutions of compact step-up voltage supply, the cascaded charge pumps has been a particular field of investigations in research activities [1,2] because of its important integration capability. Several architectures already exist such as voltage doublers [3], Dickson charge pump [4] [5], Makowsky charge pump and each of them presents different advantages about global size, efficiency, voltage gain, noise source etc. However, these solutions are typically used in low step-up voltage applications (cell phone LED camera).

A hybrid solution has been proposed in [6] by combination of Pulse Width Modulator, low-noise boost converter and a Dickson voltage multiplier for high voltage applications. Typically dedicated to comb-drive actuators, the output voltage is controlled between 10 to 300V. This compact solution is composed of a DC/DC converter. This first stage is efficient but shows relatively high power dissipation compared to the load power.

In order to investigate alternative solution for compact high voltage supply, this paper deals with the presentation of step-up voltage converter based on piezoelectric transformers dedicated to this specific application.

The power stage must convert DC voltage provided by button-cell battery to more than one hundred volts. The mems actuator used in this study involves a maximal voltage level at 120V and operating frequency close to 1kHz. The Figure 1 shows the electrostatic actuator included inside its packaging (overall size: 6800x3900x600 $\mu$ m).



Fig. 1. Electrostatic MemS inside its packaging

The electrostatic actuator is realized by the Silmach Company, obtained by lithography on SOI substrate. Its nominal functioning requires a periodic ramp waveform voltage with amplitude higher than one hundred volts at around 1-2kHz.

Note that if this actuator presents moderate electrical requirements, the power stage presented in this paper is able to provide highest voltage level and frequency. Since few years, piezoelectric transformers have been extensively distributed in place of conventional electromagnetic transformers, essentially dedicated to low power applications and embedded systems. Due to the resonant behaviour of piezoelectric transformers, many converter topologies have been studied, generally including phase control or frequency control in order to track the optimal efficiency [7], particularly for low voltage applications with important load variations. These solutions are often complex and bulky, and in contradiction with an efficient miniaturization and a low cost solution.

This paper presents an original electronic circuit, leading to its experimental validation and thereby highlights the interest of piezoelectric solutions for high voltage mems supply. The electronic circuit is presented in Section II and experimental results are discussed in Section III. Finally, the miniaturization of the Rosen type piezoelectric transformer solved by algorithmic method is briefly introduced.

## II. ELECTRONIC ARCHITECTURE

### A. The piezoelectric transformer

Among the various types of piezoelectric transformers (PT), the Rosen type presents high voltage ratio and it is typically adapted to high step-up voltage converter at low power [7][8]. This classical piezoelectric transformer operates using a longitudinal vibratory mode along the main dimension  $x_1$ . Its geometry is illustrated on Figure 2.

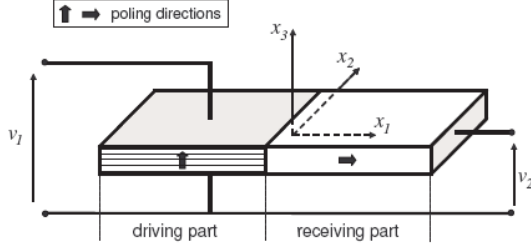


Fig. 2. Classical Rosen type transformer

It is usually composed of a laminated driving part operating in transverse mode ( $k_{31}$  coupling factor), and a receiving part in longitudinal mode ( $k_{33}$ ). The number of layers and the difference between electromechanical coupling factors of each side confer a high voltage gain. However, the relative weak value of  $k_{31}$  coupling factor implies a limited power density compared to other transformers ( $5\text{-}10\text{W}/\text{cm}^3$ ) [7], but still in the framework of expected requirements.

Stable oscillation must be maintained close to the mechanical resonance frequency of the PT in order to reach a significant voltage gain and optimal efficiency. As consequence, the resonant behaviour of the transformer must be clearly identified. For the experimental validation, a common transformer distributed by Panasonic (EFTU14R0M03A) is used. Its electrical characterization is undertaken by classical admittance analysis and identified to an electrical equivalent model (figure 6-a). Its dimensions and identified equivalent components are collected in table I. Note that at this stage of the study, dimensions of this transformer are not convenient for miniaturized system.

TABLE I  
DIMENSIONS AND EQUIVALENT PARAMETERS OF THE STUDIED PT

Dimensions		
w	width	6mm
L	length	30mm
e	thickness	2mm

Symbol	Definition	Value
N	Ideal voltage gain	48
$C_m$	Motion arm capacitance	$2.42\text{nF}$
$L_m$	Motion arm inductance	$3.59\text{mH}$
$R_m$	Motion arm resistance	$4\Omega$
$C_{d1}$	Input capacitance	$139.4\text{nF}$
$C_{d2}$	Output capacitance	$10.8\text{pF}$
$R_{d2}$	Output resistance	$8.81\text{M}\Omega$
$R_{d1}$	Input resistance	$243\Omega$

Simulations of the electrical equivalent circuit are compared to the practical results obtained at operating voltage level and illustrated on Figure 3 and Figure 4.

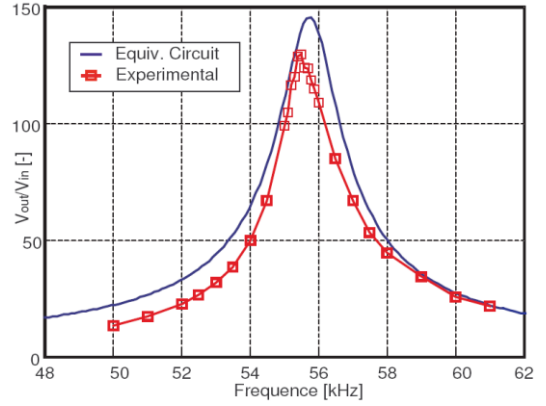


Fig. 3. Voltage gain vs frequency at constant  $R_{load}=1\text{M}\Omega$

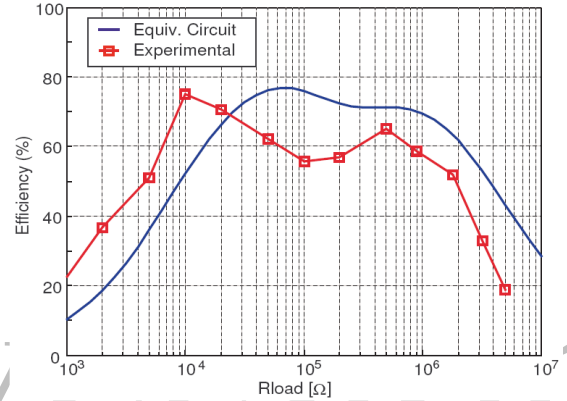


Fig. 4. PT efficiency depending on  $R_{load}$  at resonant frequency

Besides the convenient accuracy of the equivalent circuit simulations, these results show a tight resonance characteristic of voltage step-up ratio and a strong dependence of efficiency with the load variations.

About latter aspect, it may be considered as first approximation that load current consumption is sufficiently weak and constant to not influence the electrical behaviour of the transformer. In consequence, solution of self-resonant oscillator is chosen and explained below.

### B. Self-Resonant oscillator

Many papers in literature relate the necessity to control the frequency in order to track the efficient operating point [9]. Commonly, feedback methods using voltage sensors, current sensors or piezo-sensor are used. These feedback systems are particularly dedicated to relative high power applications with load variations (ex: LCD backlights).

The solution presented in this paper is initially deduced from classical Pierce resonant oscillator. However, self-oscillator circuit with piezo transformer can not be treated like quartz oscillator, due to the high output impedance of the circuit, leading to instability and weak available output power.

Even if the structure presented on figure 5 slightly differs from a classical Pierce circuit, it relies on the same principle. A stable oscillation is obtained if the feedback loop satisfies the Barkhausen criteria:

- the open loop gain exceeds unity at resonant frequency ,
- phase shift around the loop is  $2\pi.n$  radians (n is an integer).

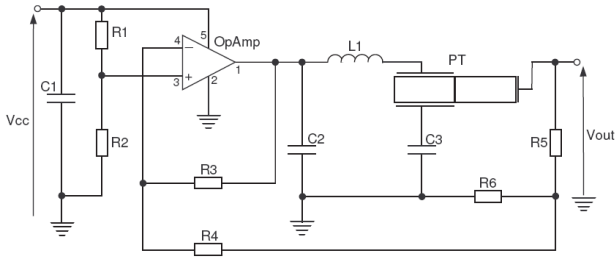


Fig. 5. Circuit based on Pierce Resonant oscillator

The first condition is easily reached using operational amplifier (or transistor amplifier) and natural high gain of PT at its resonant frequency. The stabilisation of oscillations is commonly satisfied by saturation of the amplifier. Maximal voltage level is provided to the PT input by a rail-to-rail amplifier with high bandwidth (>500kHz), low voltage supply (3V) and low current consumption (<1mA).

The second condition is essential for steady state oscillation and also fast start-up. The operational amplifier is connected as an inverting amplifier ( $\pi$  phase shift). Added to the PT behaviour and the additional network components, the second condition of  $2\pi$  phase shift is satisfied.

C3 and L1 constitute the matching input network to provide inductive (or resistive) behaviour at Opamp output [9] and satisfy the convenient phase conditions at the expected frequency avoiding the possible frequency jumping.

Due to the high output impedance circuit, the feedback is satisfied by high voltage divider from the receiving part of the transformer. Unfortunately, this simple solution constitutes an additional resistive load.

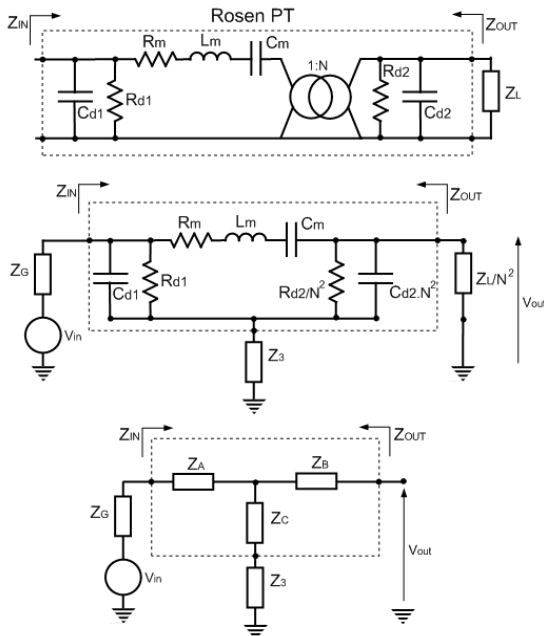


Fig. 6.  $\Pi$  to T tuned network conversion

Tuned network components must be deduced in order to satisfy the Barkhausen criteria previously mentioned and maximal voltage gain of the transformer. To do so, the

electrical equivalent circuit is modified as illustrated on Figure 6.  $Z_A$ ,  $Z_B$  and  $Z_C$  are the complex impedances after conversion from  $\Pi$  to T networks illustrated on figure 6-c.  $Z_G$  and  $Z_3$  are respectively the input inductance  $L_1$  and the series capacitance  $C_3$ .

The voltage transfer function expressed from these rearranged terms is:

$$H(s) = \frac{N \cdot Z_B}{Z_B + Z_G + Z_3 + Z_A} \quad (1)$$

The oscillation frequency must satisfy the maximal output voltage of the transformer which depends on the output load. The following demonstration will be developed by considering a resistive load.

The pulsation  $\omega_0$  of the maximal step-up voltage ratio is obtained by solving the equation below [10]:

$$\lambda^3 + \left( \frac{1}{2Q_m^2} + \frac{Q_i^2}{2} - 1 - \frac{1}{\delta} \right) \lambda^2 - \frac{Q_i^2}{2} = 0 \quad (2)$$

Then, it becomes possible to deduce the values of matching network components by solving the transfer function for a  $\pi$  phase shift condition. This implies the following approximation of  $C_3$ :

$$C_3 \approx \frac{C_{d1} \eta^2 - C_m \eta + \frac{\lambda}{\omega_s Q_m} \left( C_m \cdot Z + \frac{C_{d1}}{\omega_s Q_m} \right)}{\left( \eta^2 + \frac{\lambda}{Q_m} \right) \left( C_{d1} L_1 \omega_0^2 - 1 \right) - L_1 C_m \omega_0^2 \left( \eta - \frac{\lambda Z}{\omega_s Q_m} \right)} \quad (3)$$

with,

$$\omega_s = \frac{1}{\sqrt{L_m C_m}}, \text{ the series resonant frequency}$$

$$Q_m = \frac{1}{R_m} \sqrt{\frac{L_m}{C_m}}, \text{ the mechanical quality factor}$$

$$Q_i = C_{d2} R_{load} \omega_s, \text{ the electrical quality factor}$$

$$\delta = \psi^2 \frac{C_{d2}}{C_m}$$

$$\lambda = \frac{\omega_0^2}{\omega_s^2} \text{ and } \eta = \lambda - 1$$

$$Z = R_{load} \left( \frac{C_{d1}}{N^2} - C_{d2} \right)$$

The approximation of equation 3 is acceptable provided that the electrical quality factor is close to 1 as follow:

$$Q_i = C_{d2} R_{load} \omega_s \approx 1 \quad (4)$$

This simple relation intimately relates the electro-mechanical properties of the transformer (series resonant frequency and receiving part capacitance) with a specific load value. It describes implicitly the optimal condition to use the

transformer and consequently the necessity to select it according to the expected load.

Finally, voltage divider and inverter Opamp gain are simply deduced in order to obtain a transfer function gain slightly higher than 1.

### C. High voltage Rectifier and current source

The studied electrostatic actuator requires single-polarity pulses with a voltage ramp waveform at a maximal frequency around 2kHz. The high voltage provided by self-oscillator circuit is preliminary rectified to DC voltage by single Dickson charge pump stage. This Dickson charge pump enables to double the DC voltage level. Consequently, this voltage doubler stage contributes to reduce the technical requirements of the transformer (less step-up voltage ratio required) leading to reduce its size and number of laminated layers.

Then, the voltage ramp waveform is built on the mems capacitor supplied by current mirror circuit. The circuit connected to the oscillator output is presented on figure 8.

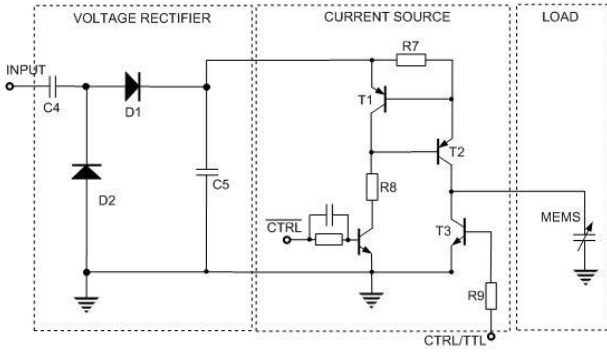


Fig. 7. Voltage rectifier and current mirror

Obviously, the components values are chosen with respect of impedance, load current and acceptable ripple voltage. The  $C_5$  capacitor permits the partial decoupling of self-oscillator with load. Its dimensioning is consequently carried out by the outgoing charges toward the load. Considering that output is composed by a current source, the minimal value of  $C_5$  capacitor is imposed by following equation:

$$q_{in}(t) \geq q_{out}(t)$$

$$C_5 \cdot V_{C5} \geq \int_0^T i_{out}(t) dt \quad (5)$$

$$C_5 \geq \frac{2 \cdot T \cdot V_{BE-T1}}{R_7 \cdot V_{C5}}$$

With  $q_{in}(t)$  and  $q_{out}(t)$  are the charge and discharge quantities in  $C_5$  capacitor respectively,  $i_{out}(t)$  is the resulting output current,  $V_{BE-T1}$  the base-emitter voltage drop of the transistor  $T_1$ ,  $V_{C5}$  the resulting constant voltage of  $C_5$  and  $T$  the turn-on period of the current source driven by CTRL/TTL command. The CTRL/TTL command permits to turn-off the current source in order to avoid unnecessary current consumption during half period.

## III. EXPERIMENTAL RESULTS

The complete electronic structure presented above is experimentally validated by a first prototype on Figure 8. Note that significant miniaturization has not been considered yet at this step of the study.

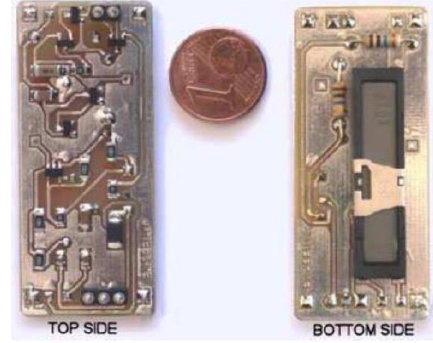


Fig. 8. Prototype of step-up voltage converter with discrete components

Figure 9 illustrates the different voltage levels of the self-oscillator stage. The amplifier output voltage is filtered correctly by the equivalent LC input impedance constituted by the tuned network.

The output voltage level of the transformer is in accordance with the characteristic on figure 3 at the operating frequency of 57.1kHz. This frequency has been fixed by the choice of  $C_3$  and  $L_1$  components in order to satisfy the expected step-up ratio, leading to oscillates at slightly highest frequency than optimal ones.

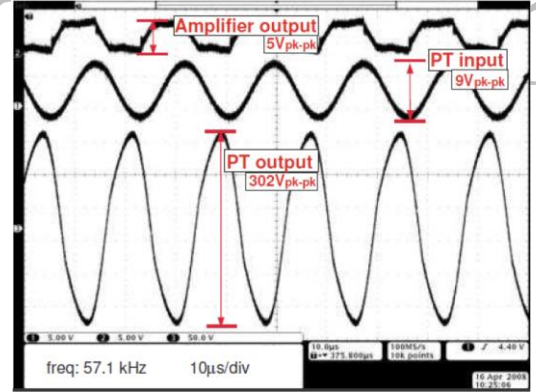


Fig. 9. Experimental voltage waveforms of self-oscillator stage

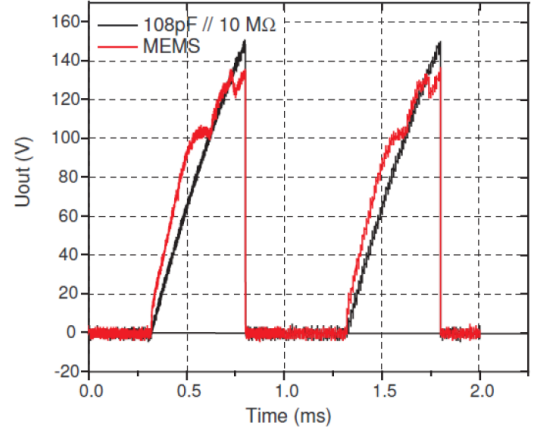


Fig. 10. Experimental output voltage

Finally, the resulting voltage applied to the micro-actuator presents the voltage waveform on figure 10 as expected.

A correct ramp waveform is obtained when the load consists on a classical capacitor. But in case of mems load, the moveable arms imply a dynamic variation of the equivalent capacitance and distortions of the voltage ramp waveform appear. Be that as it may, these small voltage drops induced by the mechanical movements illustrated on Figure 10 show an acceptable disturbance.

Obviously, the presented method for ramp waveform generation implies a constant slope coefficient and limits consequently the frequency range by the CTL/TTL command. Indeed, the frequency increasing leads to reduce the maximal voltage level reached whereas the frequency decreasing leads to the voltage ramp saturation.

#### IV. MINIATURIZED PIEZOELECTRIC TRANSFORMER

After the experimental validation of the electronic structure detailed above, a miniaturization is undertaken about the most cumbersome part which is constituted by the piezoelectric transformer.

The miniaturization procedure is based on a deterministic and rational way to design piezoelectric transformers, considering simultaneously the optimization criterion (minimal size) and electrical requirements. Indeed, resonant frequency, voltage ratio, acceptable temperature rise, etc, are some properties strongly dependent on the dimensioning, the shape, and electro-mechanical properties. Consequently, a rational method is necessary to extract the optimal performances. To do so, a deterministic methodology relying on interval arithmetic has been developed for optimization of electromechanical devices and recently for piezoelectric transformers [11].

Contrary to a common analytical method for the PT dimensioning, the selected approach lets free of arbitrary choices such as for example the resonant frequency value. Indeed, the fixing of this parameter able to simplify the dimensioning problem (reducing the degrees of freedom) but it limits strongly the field of optimal solutions. On the contrary, a frequency range is necessary in the present method and its upper bound value is deduced from the Opamp bandwidth. In the same way, the dimensions ranges are deduced from the technical limits in manufacturing.

Algorithmic methodology could not be presented in the present paper but more details are available on [11]. The solving of optimisation problem is based on an analytical model of the Rosen piezoelectric transformer fully presented in [12]. Thus, conditions of optimisation are collected in following table II.

Note that the set of constraints is defined by intervals, enabling to satisfy as well as possible the opposing criteria. The constraints on related dimensions are necessary in order to promote the convenient vibratory behaviour of the transformer. Finally, the objective function is to minimize the transformer area satisfying simultaneously the set of constraints.

TABLE II  
CONSTRAINTS AND OBJECTIVE OF OPTIMISATION

Electrical requirements		
$\omega_0$ (kHz)	Series resonant frequency	$2 < \omega_0 < 500$
$Q_i$	Electrical quality factor	$0.9 < Q_i < 0.1$
N	Voltage gain	$40 < N < 60$
$\eta_{max}$ (%)	Maximal efficiency	$90 < \eta_{max} < 100$
$R_{load}$ ( $\Omega$ )	Operating resistive load	$1.10^6$
Dimensions bound values		
w (mm)	width	$1.5 < w < 10$
L (mm)	length	$2 < L < 10$
t (mm)	thickness	$0.5 < t < 5$
n	Number of laminated layers	$1 < n < 20$
Constraints on dimensions		
$w < L/2$		
$t < w/2$		
Objective function		
Min(w×L)		

Results of optimisation are collected in table III and comparison of transformers size is shown on figure 11.

TABLE III  
RESULTS OF PT OPTIMISATION

Dimensions		
w (mm)	width	1.5
L (mm)	length	12
t (mm)	thickness	0.5
n	Number of laminated layers	6
Symbol	Definition	Value
N	Ideal voltage gain	41
Cm	Motion arm capacitance	0.344 nF
Lm	Motion arm inductance	1.31 mH
Rm	Motion arm resistance	21 $\Omega$
Cd1	Input capacitance	6.56 nF
Cd2	Output capacitance	0.74 pF

By observing the results in Table III, it can be easily observed that lower bound values have been reached for the width and thickness of PT, leading to the conclusion that smaller size may be possible if manufacturing process is improved.

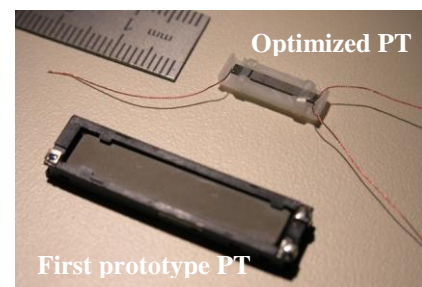


Fig. 11. Comparison of first prototype transformer and optimized version

In conclusion, these results highlight the possibility to realize compact transformer with high voltage ratio when rational and global deterministic method is used. In addition, this study has been done with Rosen type transformer, but specific efforts may be provided to define a better adapted geometry.

## V. CONCLUSION

New generation of micro-actuators has led to improve their mechanical performances and so their field of applications. However, the integration of these micro-systems is still limited by the power stage size and high step-up voltage requirements. Therefore, this paper deals with an electronic circuit developed around a high step-up piezoelectric transformer. The objective has been to demonstrate the ability to provide output voltage greatly over one hundred volts from classical cell battery voltage level. The electronic architecture relies on self-oscillator stage around the piezoelectric transformer, connected to Dickson charge pump and current source for the voltage waveform adaptation. The conditions of stable oscillation and high voltage output have been presented, leading to the calculation of matching network components. Then, experimental validation has been undertaken and has shown convenient voltage conversion. At this step of the study, efficiency and miniaturization have been considered as underlying targets and the proposed electronic circuit points to favourable criteria about these.

Finally, in order to show the miniaturization capability, the optimal dimensioning of piezoelectric transformers has been briefly introduced relying on deterministic algorithmic method. It has led to significant minimisation of the transformer size more in agreement with the expected overall size.

## REFERENCES

- [1] J.F. Richard, and Y. Savaria, "High voltage charge pump using standard CMOS technology", *Circuits and systems, NEWCAS 2004*, 2nd annual, pp 317-320, Jun. 2004.
- [2] Y.C. Cheng, C.L. Dai, C.Y. Lee, P.H. Chen, and P.Z. Chang, "A MEMS micro-mirror fabricated using CMOS post-process", *Sensors and Actuators A*, pp 573-581, 2005.
- [3] J.A. Starzyk, Y.W. Jan, and F. Qiu, "A DC-DC charge pump design based on voltage doublers", *IEEE transactions on circuits and systems*, vol 48-3, pp 350-359, 2001.
- [4] J.F. Dickson, "On-chip high-voltage generation in MNOS integrated circuits using an improved voltage multiplier technique", *IEEE journal of solid-state circuits*, vol SC-11 3, pp 374-378, 1976.
- [5] V. Jimenez, J. Pons, M. Dominguez, A. Bermejo, L. Castaner, H. Nieminen, and V. Ermolov, "Transient dynamics of a MEMs variable capacitor driven with a dickson charge pump", *Sensors and Actuators A*, (128), pp 89-97, 2006.
- [6] J.F. Saheb, J.F. Richard, R. Meingan, M. Sawan, and Y. Savaria, "System integration of high voltage electrostatic mems actuators", *IEEE-NEWCAS 2005, 3<sup>rd</sup> international*, pp 155-158, Jun. 2005.
- [7] C.A. Rosen, "Ceramic transformers and filters", *Proc. Electronic components symposium*, pp 205-211, 1956.
- [8] E.L. Hurlsey, M.P. Foster, and D.A. Stone, "State-of-the-art piezoelectric transformer technology", *European Conference on Power Electronics and Applications*, pp 1-10, Sept. 2007.
- [9] M. Sanz, P. Alou, R. Prieto, J.A. Cobos, and J. Uceda, "Comparison of alternatives to drive piezoelectric transformers", *IEEE Applied power electronics conference (APEC'02)*, vol.1, pp 358-364, Mar. 2002.

- [10] G. Ivensky, I. Zafrany, and S. Ben-Yaakov, "Generic operational characteristics of piezoelectric transformers", *IEEE transactions on power electronics*, vol.17, n°6, Nov. 2002.
- [11] F. Pigache, F. Messine, and B. Nogaede, "Optimal design of piezoelectric transformers: a rational approach based on an analytical model and a deterministic global optimization", *IEEE transactions on ultrasonics, ferroelectrics and frequency control*, vol. 54, pp 1293-1302, 2007.
- [12] S.T. Ho, "Electromechanical model of a longitudinal mode piezoelectric transformer", *7th International Conference on Power Electronics and Drive Systems, PEDS '07*, pp 267-272, 2007.

author version